Article

Utilizing the Lability of Lead Selenide to Produce Heterostructured Nanocrystals with Bright, Stable Infrared Emission

Jeffrey M. Pietryga, Donald J. Werder, Darrick J. Williams, Joanna L. Casson, Richard D. Schaller, Victor I. Klimov, and

J. Am. Chem. Soc., **2008**, 130 (14), 4879-4885 • DOI: 10.1021/ja710437r

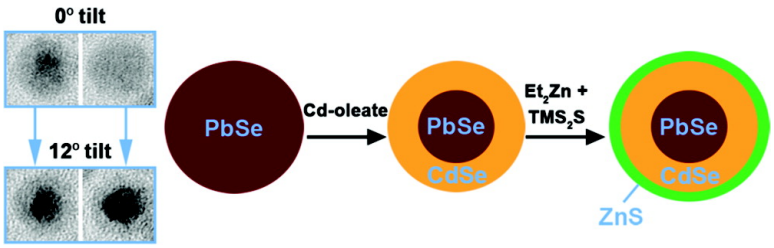

More About This Article

Additional resources and features associated with this article are available within the HTML version:

- Supporting Information
- Links to the 4 articles that cite this article, as of the time of this article download
- Access to high resolution figures
- Links to articles and content related to this article
- Copyright permission to reproduce figures and/or text from this article

View the Full Text HTML

J|A|C|S
ARTICLES
Published on Web 03/15/2008

Utilizing the Lability of Lead Selenide to Produce Heterostructured Nanocrystals with Bright, Stable Infrared Emission

Jeffrey M. Pietryga,[†] Donald J. Werder,[†] Darrick J. Williams,[‡] Joanna L. Casson,[†] Richard D. Schaller,[†] Victor I. Klimov,[†] and Jennifer A. Hollingsworth*,[†]

Chemistry Division and Center for Integrated Nanotechnologies, Los Alamos National Laboratory, Los Alamos, New Mexico, 87545

Received November 19, 2007; E-mail: jenn@lanl.gov

Abstract: Infrared-emitting nanocrystal quantum dots (NQDs) have enormous potential as an enabling technology for applications ranging from tunable infrared lasers to biological labels. Notably, lead chalcogenide NQDs, especially PbSe NQDs, provide efficient emission over a large spectral range in the infrared, but their application has been limited by instability in emission quantum yield and peak position on exposure to ambient conditions. Conventional methods for improving NQD stability by applying a shell of a more stable, wider band gap semiconductor material are frustrated by the tendency of lead chalcogenide NQDs toward Ostwald ripening at even moderate reaction temperatures. Here, we describe a partial cation-exchange method in which we take advantage of this lability to controllably synthesize PbSe/CdSe core/shell NQDs. Critically, these NQDs are stable against fading and spectral shifting. Further, these NQDs can undergo additional shell growth to produce PbSe/CdSe/ZnS core/shell/shell NQDs that represent initial steps toward bright, biocompatible near-infrared optical labels.

Introduction

Semiconductor nanocrystal quantum dots (NQDs) have been the subject of study for numerous applications requiring bright, stable fluorophores, including LEDs, lasers, detectors, and optical labels.[1−4] Much of the published work focuses on NQDs emitting in the ultraviolet and visible energy ranges, where NQDs have been posited as superior replacements for current technologies, such as organic dyes, with advantages in photostability and broad-band excitation. However, the potential impact of NQDs emitting in the infrared (IR) is much greater as the current selection of infrared fluorophores is very limited. Organic IR dyes have low photoluminescence (PL) efficiencies and are largely confined to wavelengths <1000 nm. IR-emitting rare-earth compounds offer only limited emission wavelengths and require sensitization due to characteristically small absorption cross sections.[5] Efficient, size-tunable, and broadly excitable IR NQDs thus represent not simply an incremental improvement but a fundamentally new, enabling technology.

Among narrow band gap semiconductor materials, the lead chalcogenides (PbE, E = S, Se, or Te), in particular lead selenide (PbSe), have shown the most potential as fluorophores. Facile syntheses of PbSe NQDs with photoluminescence (PL) from the near-IR as blue as 1200 nm[6−8] to the mid-IR as red as 4000 nm[9] have been reported. Further, over this range PbSe NQDs offer the highest efficiencies of any material, especially near the telecom range (1300−1550 nm), where quantum yields (QYs) approach unity and amplified spontaneous emission has been demonstrated.[10] Recently, PbSe NQDs have received even more attention for exhibiting efficient "carrier multiplication,"[11] a phenomenon in which absorption of a single, high-energy photon has produced as many as seven electron−hole pairs.[12] The harnessing of this effect could potentially revolutionize solar cell technology.

Forestalling the full application of PbSe and other lead chalcogenide NQDs, either as labels or in devices, is their inherent instability under ambient conditions. PbSe NQDs exhibit spontaneous and irreversible PL peak blue shifting (i.e., shifting to shorter wavelengths), accompanied by reduction in emission QY, over a period of days when stored in air.[13] These spectral changes may be due to destructive oxidative processes

[†] Chemistry Division.
[‡] Center for Integrated Nanotechnologies.

(1) Achermann, M.; Petruska, M. A.; Koleske, D. D.; Crawford, M. H.; Klimov, V. I. *Nano Lett.* **2006**, *6*, 1396−400.
(2) Klimov, V. I.; Bawendi, M. G. *MRS Bull.* **2001**, *26*, 998−1004.
(3) Somers, R. C.; Bawendi, M. G.; Nocera, D. G. *Chem. Soc. Rev.* **2006**, *36*, 579−91.
(4) Medintz, I. L.; Tetsuo, H. U.; Goldman, E. R.; Mattoussi, H. *Nat. Mater.* **2005**, *4*, 435−36.
(5) Klink, S. I.; Keizer, H.; van Veggel, F. C. J. M. *Angew. Chem., Int. Ed.* **2000**, *39*, 4319−21.
(6) Murray, C. B.; Sun, S.; Gaschler, W.; Doyle, H.; Betley, T. A.; Kagan, C. R. *IBM J. Res. Dev.* **2001**, *45*, 47−55.
(7) Du, H.; Chen, C.; Krishnan, R.; Krauss, T. D.; Harbold, J. M.; Wise, F. W.; Thomas, M. G.; Silcox, J. *Nano Lett.* **2002**, *2*, 1321−4.
(8) Wehrenberg, B. L.; Wang, C.; Guyot-Sionnest, P. *J. Phys. Chem. B* **2002**, *106*, 10634−40.
(9) Pietryga, J. M.; Schaller, R. D.; Werder, D.; Stewart, M. H.; Klimov, V. I.; Hollingsworth, J. A. *J. Am. Chem. Soc.* **2004**, *126*, 11752−3.
(10) Schaller, R. D.; Petruska, M. A.; Klimov, V. I. *J. Phys. Chem. B* **2003**, *107*, 13765−8.
(11) Schaller, R. D.; Klimov, V. I. *Phys. Rev. Lett.* **2004**, *92*, 186601/1−4.
(12) Schaller, R. D.; Sykora, M.; Pietryga, J. M.; Klimov, V. I. *Nano Lett.* **2006**, *6*, 424−9.
(13) Pietryga, J. M.; Casson, J. L.; Schaller, R. D.; Klimov, V. I.; Hollingsworth, J. A. *Prepr. Pap−Am. Chem. Soc., Div. Fuel Chem.* **2007**, *52*, 822−3.

Scheme 1. Synthesis of PbSe/CdSe and PbSe/CdSe/ZnS NQDs

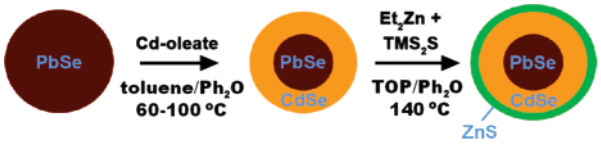

occurring at the NQD surface, possibly accompanied by dissolution. The role of oxidation is supported by both the constancy of spectral features of NQDs stored under inert atmosphere and recent spectroscopic evidence of oxidation products.[14] In this model, as oxidation proceeds from the surface inward, the effective size of the remaining PbSe domain decreases, causing an increase in confinement energy and, therefore, the observed blue shift. It has been postulated that growth of a protective "shell" of a more stable material onto the surface of the PbSe NQDs could prevent this oxidation and stabilize the nanoparticle. Recent studies have shown that a PbS shell appears insufficient to result in substantial stability enhancement.[15] In fact, evidence that PbS NQDs are also prone to oxidation has been reported previously.[16] Here, we report a novel method which takes advantage of the reactivity of PbSe NQD surface to produce PbSe/CdSe core/shell NQDs (Scheme 1). These new heterostructured NQDs combine the narrow band gap and high efficiency of PbSe NQDs with the chemical stability imparted by a CdSe shell. Further, we prove the chemical utility of the new core/shell nanocrystals by performing additional shell growth to create PbSe/CdSe/ZnS core/shell/shell NQDs (Scheme 1). These represent the first multishell architectures based on PbSe and vastly increase the relevance of PbSe-based NQDs for biolabeling applications, as an ZnS outer shell has been shown to significantly reduce cytotoxic effects of heavy-metal-bearing NQDs.[17,18]

Experimental Section

General Considerations. All syntheses were performed under exclusion of air and moisture using standard Schlenk techniques up until reaction quenching. Postpreparative handling and spectroscopy were conducted under ambient conditions. Oleic acid (Aldrich, 90%), 1-octadecene (Acros, 90%), phenyl ether (Acros, 99%), lead(II) oxide (PbO, Alfa Aesar, 99.9995%), trioctylphosphine (TOP, Strem, 97%), di-*i*-butylphosphine [$(i\text{-Bu})_2$PH, Strem, 98+%], selenium shot (Alfa Aesar, 99.999%), cadmium oxide (CdO, Strem, 99.999%), dimethyl zinc (Alrich), and hexamethyldisilathiane (Aldrich) were used without additional purification. Trioctylphosphine selenium (TOPSe) solutions of different concentrations were prepared in advance of use by heating the appropriate amounts of TOP and selenium shot to 120 °C and stirring until dissolved.

Synthesis of PbSe/CdSe Core/Shell Nanocrystals. *PbSe Cores.* A 0.65 g (2.9 mmol) amount of PbO, 2.7 mL (8.5 mmol) of oleic acid, 3 mL of trioctylphosphine (TOP), and 4 mL of phenyl ether were heated to 150 °C with stirring under flowing Ar for 90 min. The temperature was increased to 205 °C, and 2 mL of a 2 M solution of TOPSe in TOP and ~0.05 mL $(i\text{-Bu})_2$PH were rapidly injected. The reaction was quenched after 100 s by removal from heat and injection of cold toluene (~10 mL) and then hexane (~5 mL). PbSe NQDs were collected by precipitating with 15 mL of methanol followed by centrifugation and removal of the decantate. The very dark brown NQD solids were redispersed in ~8 mL of hexane, and a portion was set aside for spectroscopy and other analyses. Before CdSe shell growth, the cores were washed one additional time by precipitating by addition of 5 mL of acetone and 5 mL of methanol, centrifugation, and removal of the decantate. Approximately 100 mg of solid product was formed.

CdSe Shell. A 1.5 g (11.7 mmol) amount of CdO, 9 mL (28.3 mmol) of oleic acid, and 22 mL of 1-octadecene were heated to 255 °C under Ar until all of the CdO had dissolved. The clear solution was cooled to ~120 °C under Ar flow to remove water. A 90 mg amount of PbSe cores from above was dispersed in 10 mL of toluene and degassed by Ar flow for ~30 min. Immediately after the temperature of the PbSe solution was set to 100 °C, the cadmium oleate solution was added via cannula with stirring. Aliquots were removed and cooled by mixing with hexane, and NQDs were isolated and collected in a manner similar to that used for PbSe cores.

Synthesis of PbS/CdS Core/Shell Nanocrystals. *PbS Cores.* PbS nanocrystals with a 5 nm diameter were prepared using a slight modification of the general method described by Hines and Scholes.[19] A 0.27 g (1.2 mmol) amount of PbO, 0.8 mL (2.5 mmol) of oleic acid, 5 mL of TOP, and 10 mL of 1-octadecene were heated to 150 °C with stirring under Ar flow for 1 h. The mixture was removed from heat, and a solution of 0.1 g (0.6 mmol) of hexamethyldisilathiane in 6 mL of 1-octadecene was immediately injected. The reaction was quenched after 10 s by addition of 15 mL of cold hexane. PbS NQDs were collected by precipitating with 10 mL of methanol and 15 mL of acetone followed by centrifugation and removal of the decantate. After redispersing in ~10 mL of toluene, the NQDs were washed one additional time by the same process and redispersed once again in 12 mL of toluene. The suspended cores were used for further reaction without initial isolation as a solid as this synthetic method gives essentially quantitative yield.[19]

CdS Shell. A 1.0 g (7.8 mmol) amount of CdO, 6 mL (19 mmol) of oleic acid, and 16 mL of phenyl ether were heated to 255 °C under Ar until all of the CdO had dissolved. The clear solution was cooled to ~155 °C under Ar flow to remove water. The PbS core solution from above was degassed by Ar flow for ~30 min. Immediately after the temperature of the PbS solution was set to 100 °C, the cadmium oleate solution was added via cannula with stirring. Aliquots were removed and cooled by mixing with hexane, and NQDs were isolated and collected in a manner similar to that used for PbS cores.

Synthesis of PbSe/CdSe/ZnS Core/Shell/Shell Nanocrystals. *PbSe/CdSe NQDs.* A 1.6 g (7.2 mmol) amount of PbO, 5.5 mL (17.3 mmol) of oleic acid, 8 mL of trioctylphosphine (TOP), and 12 mL of phenyl ether were heated to 150 °C with stirring under flowing Ar for 90 min. The temperature was increased to 205 °C, and 15 mL of a 0.8 M solution of TOPSe in TOP and ~0.2 mL of $(i\text{-Bu})_2$PH were rapidly injected. The reaction was quenched after 25 s by removal from heat and injection of cold toluene (~15 mL) and then hexane (~10 mL). PbSe NQDs were collected by precipitating with 20 mL of methanol followed by centrifugation and removal of the decantate. The very dark brown NQD solids were redispersed in ~12 mL of hexane, and a portion was set aside for spectroscopy and other analyses. The PbSe cores were washed one additional time by precipitating by addition of 10 mL of acetone and 15 mL of methanol, centrifugation, and removal of the decantate. A 2.0 g (15.6 mmol) amount of CdO, 14 mL (44 mmol) of oleic acid, and 30 mL of phenyl ether were heated to 255 °C under Ar until all of the CdO had dissolved. The clear solution was cooled to ~140 °C under Ar flow to remove water. In a separate flask, the PbSe core solids were dispersed in 25 mL of toluene and degassed by Ar flow for ~30 min. Immediately after the temperature of the PbSe solution was set to 100 °C, the cadmium oleate solution was added via cannula with stirring. After 19.5 h, the reaction was removed from

(14) Sapra, S.; Nanda, J.; Pietryga, J. M.; Hollingsworth, J. A.; Sarma, D. D. *J. Phys. Chem. B* **2006**, *110*, 15244−50.
(15) Stouwdam, J. W.; Shan, J.; van Veggel, F. C. J. M.; Pattantyus-Abraham, A. G.; Young, J. F.; Raudsepp, M. *J. Phys. Chem. C* **2007**, *111*, 1086−92.
(16) Lobo, A.; Moller, T.; Nagel, M.; Borchert, H.; Hickey, S. G.; Weller, H. *J. Phys. Chem. B* **2005**, *109*, 17422−17428.
(17) Kirchner, C.; Liedl, T.; Kudera, S.; Pellegrino, T.; Javier, A. M.; Gaub, H. E.; Stolzle, S.; Fertig, N.; Parak, W. J. *Nano Lett.* **2005**, *5*, 331−338.
(18) Derfus, A. M.; Chan, W. C. W.; Bhatia, S. N. *Nano Lett.* **2004**, *4*, 11−18.
(19) Hines, M. A.; Scholes, G. D. *Adv. Mater.* **2003**, *15*, 1844−1849.

heat and the NQDs were collected as described previously and washed by one additional precipitation. Approximately 285 mg of product was formed.

ZnS Shell. A 70 mg amount of the above NQDs was dispersed in 5 mL of hexane and degassed by Ar flow. A 10 mL amount of TOP, 2 mL of oleic acid, and 20 mL of phenyl ether were added, and the solution was heated to 140 °C with Ar flow to remove the remaining hexane. A stock solution (0.03 mL [0.3 mmol] of diethyl zinc, 0.04 mL [0.2 mmol] of hexamethyldisilathiane, 1.5 mL of TOP) was added dropwise over 3.5 min. Aliquots were removed and cooled by mixing with hexane, and NQDs were isolated and collected as described above. The reaction was quenched after 22 min of total reaction time.

Results and Discussion

"Cadmium Treatment" Method. We initially attempted to grow a CdSe shell onto a PbSe NQD utilizing conventional core/shell methods. CdSe comprises a near-ideal candidate for shell growth based on a number of its properties. First, CdSe NQDs exhibit relatively higher stability under ambient conditions. Second, the much larger bulk band gap of CdSe relative to PbSe raises the probability that charge carriers remain confined to the PbSe core, resulting in effective "inorganic passivation", in a manner similar to the well-known CdSe/ZnS core/shell system.[20] Finally, the bulk lattice parameters of cubic PbSe (rock-salt) and CdSe (zinc-blende) differ by ~1%, increasing the probability of a smooth, low-defect interface between the materials. Unfortunately, the conventional paradigm for core/shell NQD synthesis in which a solution of NQD cores and the appropriate surfactant(s) is exposed to precursors containing both the anion and the cation of the "shell" material did not consistently produce the desired results. Our attempts to use cadmium oleate and trioctylphosphine selenium (TOPSe),[9] as well as other precursor combinations, were frustrated by the sensitivity of the PbSe cores to heating in solution and competitive homogeneous nucleation of very small CdSe particles.

To overcome these problems, a new approach was applied. Rather than exposing PbSe cores to both cadmium and selenium precursors, only cadmium was introduced and in excess relative to lead. Because heating PbSe in solution can cause observable Ostwald ripening at temperatures as low as 80 °C, it was expected that lead ions in the NQDs, especially those near the surface, would be susceptible to exchange with other metal ions from the solution. It was also expected that the excess cadmium and larger lattice energy of CdSe of 797 vs 730 kcal/mol would favor a net replacement of lead with cadmium over the reverse process. Further, rather than applying conditions designed exclusively to enhance ion exchange, such as use of a highly ionic precursor and a strong cation-binding solvent, which can quickly result in total replacement in some systems,[21] we sought to employ milder conditions similar to those under which Ostwald ripening might occur. Use of a relatively slow-reacting cadmium precursor, soluble in noncoordinating solvents, allowed us to shift the solution equilibrium to favor net ion substitution under more controlled conditions. It was anticipated that such gentle manipulation of the solution equilibrium would allow slow, self-limiting substitution, resulting in the desired core/shell structure.

(20) Hines, M. A.; Guyot-Sionnest, P. *J. Phys. Chem.* **1996**, *100*, 468−71.
(21) Son, D. H.; Hughes, S. M.; Yin, Y.; Alivisatos, A. P. *Science* **2004**, *306*, 1009−12.

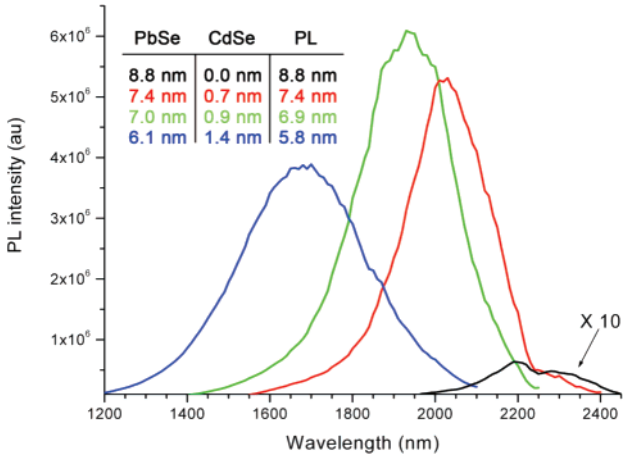

Figure 1. PL spectra from a series of aliquots during CdSe shell formation, corresponding to 15 min, 2 h, and 24 h of reaction time proceeding from red to blue. Each spectrum is corrected for variation in optical density as well as grating and detector efficiencies to reflect relative QY. Shown in black is the original PbSe core, magnified 10-fold so its shape is discernible. The inset lists the calculated core diameter (column "PbSe") and shell thickness ("CdSe") from elemental analysis. Also included is the approximate effective core size predicted by the PL peak position ("PL").

Characterization of PbSe/CdSe NQDs. Figure 1 shows a sequence of PL spectra[22] obtained from aliquots during a single core/shell synthesis. The observed shifting of PL peak position to shorter wavelengths can be explained by formation of an increasingly thick CdSe shell resulting from sacrificial replacement of lead with cadmium. Significantly, in contrast to the oxidation processes described above, this steady blue shift in PL peak position due to the decrease in the effective size of the PbSe "core" is controllable and reproducible. CdSe shell formation proceeds without significant chemical "etching" (i.e., net loss of material) or material adgrowth as the mean particle diameter of the core/shell NQDs, as determined by small-angle X-ray scattering (SAXS),[23] are typically within 2% of the mean diameter of the original PbSe particles. This is noted to be well within the normal size dispersion of 5−10% and is consistent with the substitution of cubic PbSe (lattice constant = 6.12 Å) by cubic CdSe (6.05 Å), which should result in negligible change in particle size.

The presence of cadmium and relative amount of lead and cadmium in the NQDs of each aliquot was determined by inductively coupled plasma-optical emission spectroscopy (ICP-OES).[24] As expected, the amount of cadmium increased according to the degree of PL shift, up to a Cd:Pb atomic ratio of 1.86:1 measured in the bluest-emitting aliquot. Using these ratios, the diameter of the remaining PbSe core and thickness of the CdSe shell were calculated, assuming no significant intermixing of material domains. The inset in Figure 1 shows the calculated core diameter and shell thickness for each of the

(22) PL measurements were performed on hexane or, when necessary, toluene-d_8 solutions of NQDs diluted to an optical density between 0.05 and 0.12 at the excitation wavelength. All samples were excited using an 808 nm diode laser and collected on an LN_2-cooled InSb detector with a grating monochromator. The excitation was mechanically chopped, and the signal was enhanced by a lock-in amplifier.
(23) SAXS analyses were performed on NQDs in hexane solutions with a transmission coefficient between 30% and 50% in a 1 mm capillary tube using a Rigaku Ultima III diffractometer with a Cu Kα (1.5406) X-ray source and "Nano-Solver" (by Rigaku) analysis software. The scattering range was from $2\theta = 0.1000-6.0000°$. For each sample, an empty capillary background was subtracted from the raw data prior to profile fitting.
(24) Elemental analyses were performed by Galbraith Laboratories, Inc., Knoxville, TN, 37950-1610.

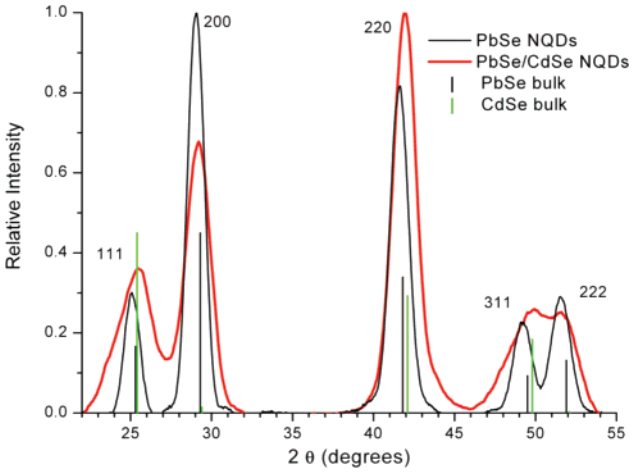

Figure 2. Powder XRD patterns of 8.8 nm total diameter PbSe and PbSe/CdSe NQDs with bulk line positions and relative intensities for rock-salt PbSe and zinc-blende CdSe.

corresponding aliquots as well as the effective core size predicted by the PL peak position. Given the simplicity of this structural model, the agreement is remarkably close, which supports the conclusion that the observed blue shifting of PL peak position results from CdSe shell formation due to sacrificial loss of lead. The slight deviation at higher thicknesses may be due to a small amount of lead alloyed into the CdSe shell, which would reduce the size of the pure PbSe core and result in bluer than predicted emission.

Although the PL and elemental analysis data support the conclusion that a core/shell structure has been produced, they cannot definitively rule out that we instead produced homogeneous $Pb_xCd_{1-x}Se$ alloyed NQDs. Indeed, the observed blue shift could alternatively be attributed to the increase in bulk band gap in going from pure PbSe to a cadmium-containing alloy, as observed in studies of bulk pure and alloy thin films.[25] In our quantum confined system this shift would be more complicated than in the bulk. The contribution to the observed band gap from confinement would also be expected to change with composition as pure PbSe and CdSe have vastly different bulk exciton Bohr radii (46 and 6 nm, respectively). To resolve this debate, the NQDs were subjected to further structural analysis.

The powder X-ray diffraction (XRD) pattern[26] of PbSe and PbSe/CdSe nanocrystals of the same total diameter are compared in Figure 2. As expected, the overall pattern for each sample remains cubic. The slightly smaller *d* spacing of CdSe results in peaks that consistently appear shifted, or more accurately broadened, toward higher 2θ. We believe this to be indicative of formation of separate, crystalline but crystallographically unrelated PbSe and CdSe domains, resulting in separate PbSe and CdSe peaks that are not resolvable due to the similarity in *d* spacing. Further evidence for this can be found in the change in the pattern of intensities, as can most strikingly be seen in comparing the 111, 200, and 220 peaks. In PbSe, a rock-salt lattice, the 200 is the principal peak followed by the 220 and then the 111. However, in CdSe, a zinc-blende lattice, the 200 is essentially absent, the 111 is the principal peak, and the 220 remains substantial (Figure 2, vertical lines). The PbSe/CdSe pattern shown in Figure 2, with a relatively thick shell (~1.5 nm), appears to be intermediate between these two extremes, implying a superposition of rock-salt and zinc-blende patterns of similar *d* spacing. Finally, the observed increase in peak broadening is likely a result not only of the superposition of the peaks of two similar materials but also of a decrease in average domain size as a result of formation of a separate CdSe shell. In contrast, a homogeneous $Pb_xCd_{1-x}Se$ NQD would possess a clearly rock-salt or zinc-blende intensity pattern, not a superposition, and not be expected to exhibit increased broadening for either of the reasons given above.

To further confirm a core/shell structure, the PbSe/CdSe NQDs were examined using transmission electron microscopy (TEM).[27] Figure 3 shows TEM images of PbSe/CdSe core/shell nanocrystals. The good lattice match makes it difficult to see the interface between the two material domains, even in high-resolution images (Figure 3a). However, the significant difference in atomic number between lead and cadmium should render any PbSe regions darker due to stronger electron diffraction. This is apparent in a few individual nanocrystals in Figure 3b. The image depicted in Figure 3c is of the same area, tilted 12° with respect to Figure 3b in order to bring a larger number of QDs into a strong Bragg condition. The enhanced contrast between the CdSe (outer shell, lighter in color) and PbSe (inner core, darker) reveals the anticipated core/shell structure. The random orientation of NQDs throughout the whole sample makes it impossible to bring them all into high contrast in a single image.

Flexibility. This CdSe shell formation procedure has been successfully applied to PbSe NQDs varying in size from 5 to over 11 nm (Figure 4) in diameter and can be used to create relatively thin CdSe shells on PbSe NQDs as small as 2 nm. It is equally applicable to NQDs of other lead chalcogenides, such as PbS (yielding PbS/CdS NQDs, Figure 5). In fact, starting with relatively small PbS cores, this method can result in PbS/CdS NQDs that emit from 800 to 950 nm (Figure 5b), a spectral range with particular advantages for biolabeling applications with respect to enhanced tissue transparency and reduced autofluorescence.[28] Interestingly, the lead replacement by our methods appears in all cases to be a self-limiting process for both PbSe and PbS NQDs, as predicted for our chosen conditions. Regardless of initial NQD diameter, the reaction does not proceed beyond a terminal shell thickness (as in the 1.5 nm shell described above) and has not been effected to completeness even with larger cadmium excesses and longer reaction times. Exposing even very small PbSe NQDs (<2 nm) to large excesses of cadmium has not, so far, resulted in NQDs emitting at wavelengths reachable by pure CdSe NQDs (<700 nm).

Optical Properties and Stability of PbSe/CdSe NQDs. The shell formation process produces noted improvement in emission efficiency, especially when applied to NQDs with low initial QY. Small, high-quality PbSe NQDs with high initial QYs (>70%) show no change or modest improvement, but larger and/or poorer quality NQDs can be markedly improved, as seen in Figure 1, in which the efficiency is >160-fold enhanced (to

(25) Hankare, P. P.; Delekar, S. D.; Chate, P. A.; Sabane, S. D.; Garadkar, K. M.; Bhuse, V. M. *Semicond. Sci. Technol.* **2005**, *20*, 257−64.
(26) XRD patterns were collected on a Rigaku Ultima III diffractometer that using a Cu Kα (1.5406 Å) X-ray source. The thick, solid NQD films were drop cast onto zero-background silicon substrates.
(27) TEM studies were done on a JEOL 2010 operating at 200 kV and a FEI Tecnai G2 30 (S)TEM operating at 300 kV.
(28) Chance, B. *Ann. N.Y. Acad. Sci.* **1998**, *838*, 29−45.

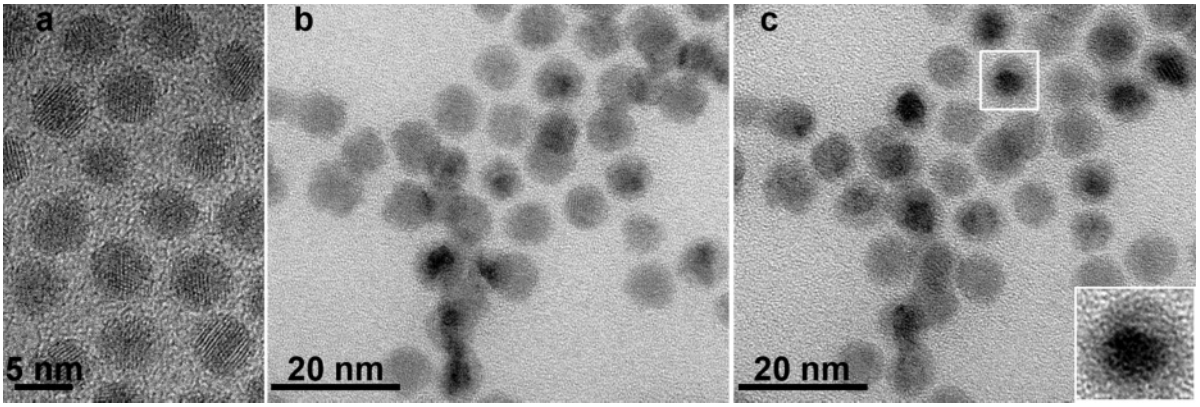

Figure 3. TEM images of PbSe/CdSe NQDs. (a) High-resolution image of NQDs with 3.0 nm diameter PbSe cores with 1.5 nm CdSe shells, showing the subtle core/shell interface. (b) Low-resolution image of 6.1 nm PbSe cores with 1.4 nm shells. (c) Low-resolution image of the same area as b, but tilted by 12° to enhance the diffraction contrast of more NQDs. Inset shows higher magnification image of a single NQD with enhanced contrast; distinct core/shell structure is apparent.

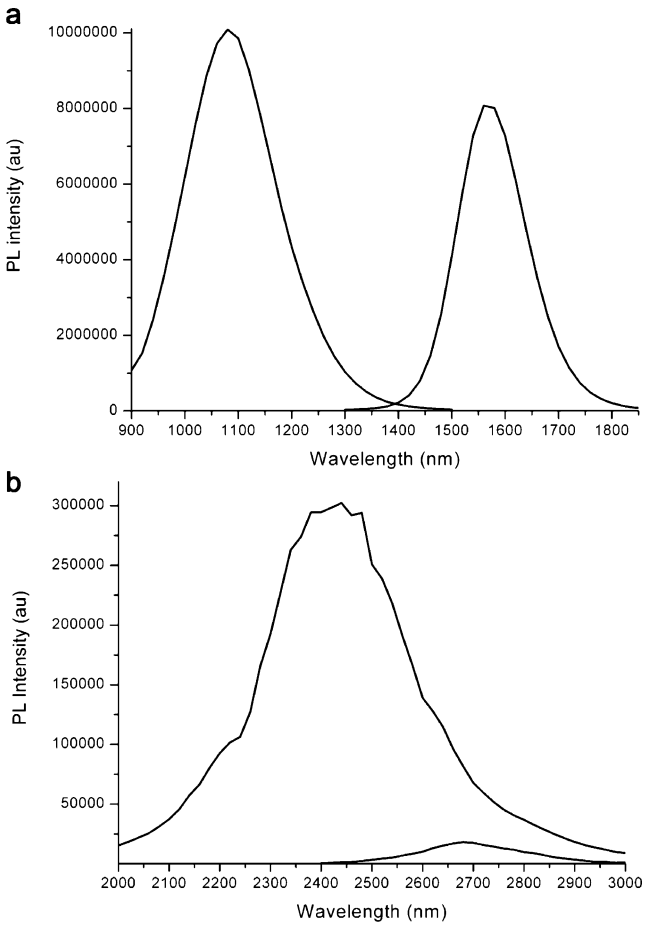

Figure 4. PL spectra of PbSe and PbSe/CdSe NQDs of different sizes: (a) 5.2 nm diameter PbSe NQDs (higher wavelengths) and corresponding PbSe/CdSe NQDs (lower wavelengths) and (b) 11.5 nm PbSe NQDs and corresponding PbSe/CdSe NQDs.

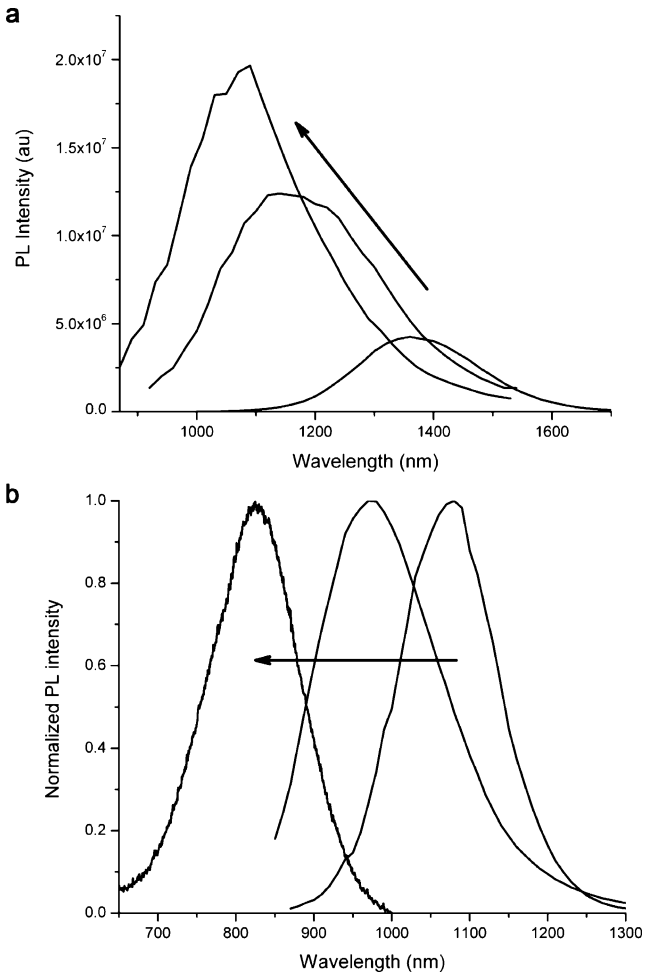

Figure 5. PL spectra of PbS and PbS/CdS NQDs. Arrows indicate progress of reaction during CdS shell formation: (a) Spectra of larger (~7 nm) PbS and two aliquots during CdS shell formation, showing relative PL enhancement during the process; (b) normalized spectra of smaller (~5 nm) PbS and PbS/CdS NQDs with PL as blue as 830 nm. The bluest spectrum was collected on an Ocean Optics USB2000 spectrometer, making direct comparison of peak intensities difficult. PL peaks have been normalized for easier comparison of position and shape. QYs for the bluest PbS/CdS NQDs are typically 20−30%.

~17% QY, in this case). Moreover, the blue shift that results from shell formation, up to the terminal thickness, is controllable in degree by variation of time, temperature, and reactant concentrations, and a large portion of the total PL enhancement is achieved at relatively thin shell thicknesses. In fact, use of low temperatures (<35 °C) can result in efficiency enhancement with minimal shift. For example, the QY of low-quality PbSe NQDs emitting initially at 1590 nm was enhanced 7-fold (to 81%) by exposure to a cadmium precursor solution at room temperature with a blue shift of only 50 nm (Figure 6). The exact structure of the enhanced NQDs created at low temperatures is the subject of a current investigation; however, they are known (as determined by energy-dispersive X-ray analysis,

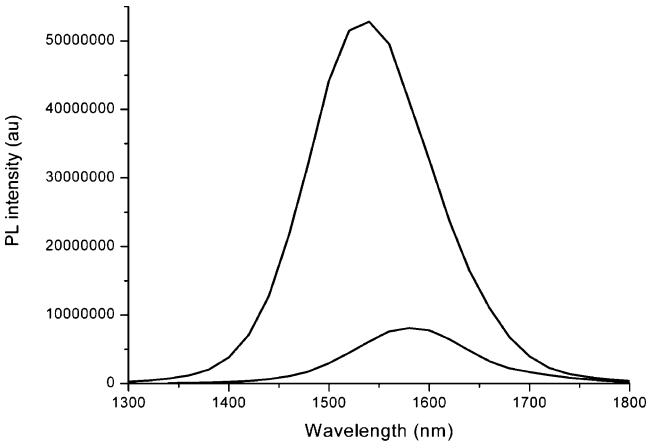

Figure 6. PL spectra of 5.2 nm PbSe NQDs before (small peak) and after (large peak) exposure to a cadmium oleate solution for 19 h at room temperature.

EDX[29]) to contain much smaller amounts of cadmium. If the shell-formation process depends on the same surface-ion lability responsible for Ostwald ripening, as we conjectured, then it is completely expected that lower reaction temperatures will result in this very limited ion exchange.

The core/shell structure of the PbSe/CdSe NQDs leaves the PbSe, previously observed to be unstable, effectively sequestered from the surrounding environment. As hoped, this results in tremendously enhanced stability. A shell of CdSe extends the useful life of PbSe NQDs under ambient conditions from a few days to at least several months, during which time the emission efficiency declines only very slowly and does not measurably shift in wavelength.[13] As was the case with the increase in PL efficiency, stability is considerably improved even with relatively thin CdSe shells. The ability to enhance both stability and efficiency is particularly relevant in the context of more recent high-chemical-yield PbSe NQD preparations.[30] Addition of small amounts of diaryl- or, we have found, dialkylphosphines to the standard reaction mixture significantly improves chemical yields (e.g., ~15% vs ~5% for 8 nm diameter NQDs). We observed that this advantage of higher yields is somewhat offset by the often lower emission efficiencies and *even greater* instability of PbSe NQDs prepared with these additives. However, by performing CdSe shell growth on such NQDs, we are able to dramatically enhance their stability and PL efficiencies, allowing us to fully reap the benefits of higher yield syntheses.

The increased stability also manifests itself in increased chemical flexibility. Following a procedure established by Lee et al.,[31] the PbSe/CdSe NQDs were successfully embedded in a castable thermoset polymer with retention of emission efficiency and energy, whereas the same process quickly degrades uncoated PbSe NQDs, presumably by reaction of the surface with the radical initiator. Finally, a CdSe shell effectively prevents Ostwald ripening even at temperatures >140 °C, opening the door for additional chemistry such as further shell growth.

(29) Elemental analyses were performed on a FEI Tecnai G2 30 (S)TEM operating at 300 KV using an EDAX EDAM III energy-dispersive spectrometer with a Si(Li) detector. FEI TIA software was used to analyze the collected data.
(30) Steckel, J. S.; Yen, B. K. H.; Oertel, D. C.; Bawendi, M. G. *J. Am. Chem. Soc.* **2006**, *128*, 13032−3.
(31) Lee, J.; Sundar, V. C.; Heine, J. R.; Bawendi, M. G.; Jensen, K. F. *Adv. Mater.* **2000**, *12*, 1102−5.

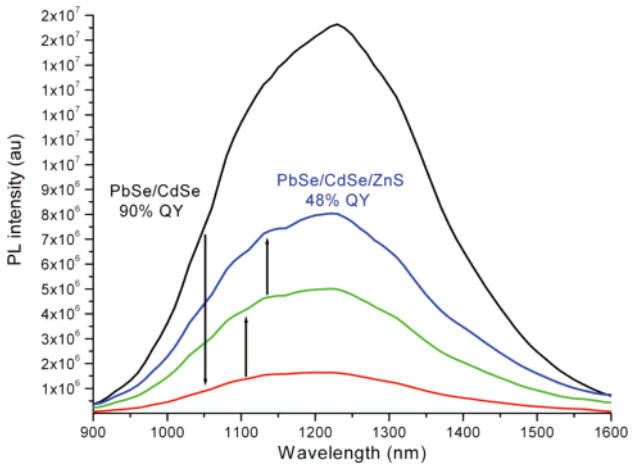

Figure 7. PL spectra of a series of aliquots taken during growth of a ZnS shell on PbSe/CdSe NQDs. Arrows denote the forward progress of the reaction.

ZnS Shell Growth. If, as we have shown, the surface of these new NQDs is composed of CdSe, it follows that they should demonstrate similar chemistry to the well-known CdSe NQDs. One of the most characteristic and potentially important chemistries of CdSe NQDs is overcoating with zinc sulfide (ZnS). Growth of a relatively thin shell of ZnS on CdSe provides effective inorganic passivation, resulting in brighter and more stable emission. In addition, the ZnS shell can serve as a barrier to dissolution of cadmium ions under biological conditions, leading to marked reduction in cytotoxicity,[17] especially cytotoxicity deriving from NQD oxidation by air.[18] In this way, CdSe NQDs have been rendered more suitable for biolabeling applications, and by analogy, addition of a ZnS shell to PbSe/CdSe NQDs should result in more biocompatible PbSe-based NQDs with the added advantages of emission in the near-infrared.

Using a slight variation of CdSe literature methods,[20] we successfully grew a ZnS shell on PbSe/CdSe NQDs (Scheme 1). Figure 7 shows the PL spectra of a series of aliquots taken during ZnS shell growth, including the original PbSe/CdSe NQD before ZnS growth. At early shell growth stages, the PL efficiency is substantially diminished, an effect not seen in a control experiment in which the NQDs are heated without added precursor. As growth continues, PL efficiency appreciably recovers until an apparent "ideal" shell thickness, after which it starts to decline again. It is not known at this point whether the fluctuation in PL is endemic or can be overcome by further refinement of the synthetic procedure. However, it is worth noting that given the very high QY of typical PbSe/CdSe NQDs, these PbSe/CdSe/ZnS multishell NQDs can still easily demonstrate QYs of near 50% even by our simple, relatively unrefined methods. Finally, in contrast to the CdSe shell formation, no shift in PL peak position is observed. This is an indication that the CdSe shell is robust with respect to Ostwald ripening processes and that the PbSe core is not susceptible to further loss of lead during ZnS shell growth, despite the increased temperature.

SAXS analysis reveals that the mean particle diameter increases, in this case, from 5.6 to 6.4 nm during ZnS shell growth. Although it was not possible to distinctly resolve the very thin shell of ZnS in TEM images (Figure 8), both zinc and sulfur were found to be present by EDX, and the magnitude

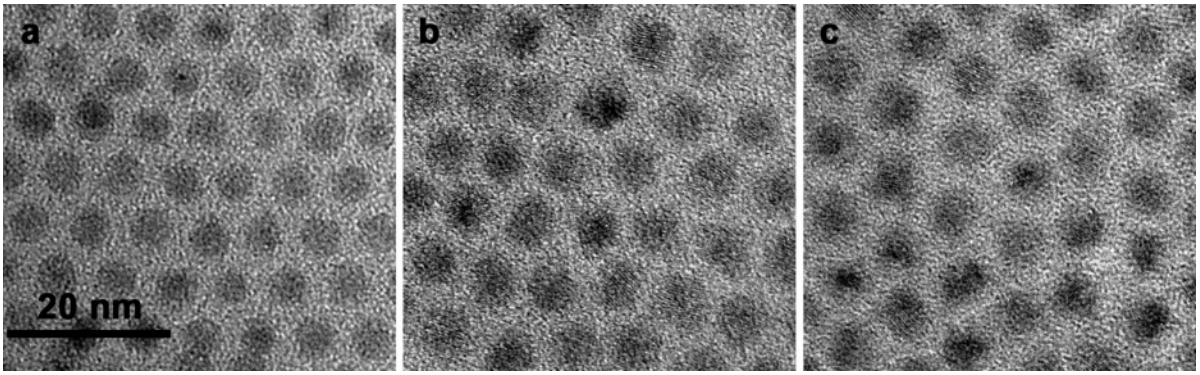

Figure 8. Series of TEM images depicting growth of ZnS shell on 5.6 nm (total) PbSe/CdSe: (a) no shell; (b) 0.3 nm shell; (c) 0.4 nm shell.

of the diameter increase was confirmed. The images also reveal that while the PbSe/CdSe/ZnS core/shell/shell particles are still spherical on average, they are slightly rougher edged, implying the ZnS shell is not uniform. This is not surprising given that the shell is only slightly thicker than one monolayer ($a = 5.41$ Å). Elemental analysis, again by ICP-OES, verified the Zn:S atomic ratio to be 1:1 and yielded an estimated shell thickness of 0.37 nm, in good agreement with the observed diameter increase. Although PbSe/CdSe/ZnS NQDs appear to be stable under ambient conditions over normal analysis time periods, as determined by PL measurements, the effect of this final shell growth on the stability of the NQDs over longer time periods is still under investigation.

Conclusions

A method for stabilizing lead chalcogenide NQDs has been sought for some time. Standard methods that were developed for the ubiquitous CdSe NQD system, such as inorganic passivation, have not proven applicable, likely due to both their divergent passivation chemistries and the instability of lead chalcogenides toward increased temperature and adverse chemical reactions. We used this instability to our advantage, however, to force the partial, surface-specific replacement of lead with cadmium, resulting in a core/shell NQD with markedly superior properties. The stability enhancement alone greatly extends the range of possible applications by removing the need for handling and storage under controlled conditions and increasing the usable temperature range. In addition to conferring stability, the CdSe shell formation process can also be used simply as a post-preparative method for enhancing PL. This allows one to use synthetic pathways that give better chemical yields but poorer initial NQD quality with the intention of using shell formation to "repair" the less-than-ideal NQDs. The controllable blue shifting endemic in the process is easily worked around, if necessary, simply by growing the original PbSe NQDs slightly larger than the desired final size. In fact, this effect can be used to synthesize PbSe/CdSe NQDs emitting at wavelengths < 1000 nm and PbS/CdS NQDs emitting as blue as 830 nm, wavelengths of particular interest for biolabeling applications. Finally, growth of a ZnS shell on these new PbSe/CdSe NQDs confirms that they can be chemically modified in the same way as CdSe NQDs, opening a host of further possibilities already established for this well-studied material, including rendering the NQDs water soluble. Further, studies are underway to compare the cytotoxicity of lead chalcogenide core-only NQDs with their core/shell and core/multishell counterparts to assess the ability of the ZnS shell in particular to reduce toxic effects associated with exposure to heavy-metal ions. With broadband absorption spectra and high emission efficiencies, these new NQDs could prove to be extremely effective and versatile optical biolabels.

Acknowledgment. This work was supported by the Intelligence Technology Innovation Center. J.M.P. was supported by an Intelligence Community Postdoctoral Research Fellowship. D.J.W., V.I.K., and J.A.H. acknowledge the support of the Center for Integrated Nanotechnologies, a U.S. Department of Energy Office of Basic Energy Sciences Nanoscale Science Research Center.

Supporting Information Available: Absorption spectra of PbSe/CdSe NQDs, full elemental analysis reports. This material is available free of charge via the Internet at http://pubs.acs.org.

JA710437R